Annals of Botany **125**: 353–364, 2020
doi: 10.1093/aob/mcz137, available online at www.academic.oup.com/aob

ANNALS OF BOTANY
Founded 1887

PART OF A SPECIAL ISSUE ON COASTAL FLOODING AND STORM RISKS

Elevated micro-topography boosts growth rates in *Salicornia procumbens* by amplifying a tidally driven oxygen pump: implications for natural recruitment and restoration

Gregory S. Fivash[1*], Jim van Belzen[1], Ralph J. M. Temmink[2], Karin Didderen[3], Wouter Lengkeek[3], Tjisse van der Heide[4,5] and Tjeerd J. Bouma[1,6,7]

[1]Department of Estuarine and Delta Systems, Royal Netherlands Institute for Sea Research and Utrecht University, Yerseke, the Netherlands, [2]Aquatic Ecology and Environmental Biology, Institute for Water and Wetland Research, Radboud University, Nijmegen, the Netherlands, [3]Bureau Waardenburg, Culemborg, the Netherlands, [4]Department of Coastal Systems, Royal Netherlands Institute for Sea Research and Utrecht University, Den Burg, the Netherlands, [5]Conservation Ecology Group, Groningen Institute for Evolutionary Life Sciences, University of Groningen, Groningen, the Netherlands, [6]Delta Academy Applied Research Centre, HZ University of Applied Sciences, Vlissingen, the Netherlands and [7]Faculty of Geosciences, Department of Physical Geography, Utrecht University, 3508 TC Utrecht, the Netherlands
** For correspondence. E-mail greg.fivash@nioz.nl*

Received: 21 March 2019 Returned for revision: 25 April 2019 Editorial decision: 7 August 2019 Accepted: 16 August 2019
Published electronically 21 August 2019

• **Background and Aims:** The growth rate of pioneer species is known to be a critical component determining recruitment success of marsh seedlings on tidal flats. By accelerating growth, recruits can reach a larger size at an earlier date, which reduces the length of the disturbance-free window required for successful establishment. Therefore, the pursuit of natural mechanisms that accelerate growth rates at a local scale may lead to a better understanding of the circumstances under which new establishment occurs, and may suggest new insights with which to perform restoration. This study explores how and why changes in local sediment elevation modify the growth rate of recruiting salt marsh pioneers.
• **Methods:** A mesocosm experiment was designed in which the annual salt marsh pioneer *Salicornia procumbens* was grown over a series of raised, flat and lowered sediment surfaces, under a variety of tidal inundation regimes and in vertically draining or un-draining sediment. Additional physical tests quantified the effects of these treatments on sediment water-logging and oxygen dynamics, including the use of a planar optode experiment.
• **Key Results:** In this study, the elevation of sediment micro-topography by 2 cm was the overwhelming driver of plant growth rates. Seedlings grew on average 25 % faster on raised surfaces, which represented a significant increase when compared to other groups. Changes in growth aligned well with the amplifying effect of raised sediment beds on a tidally episodic oxygenation process wherein sediment pore spaces were refreshed by oxygen-rich water at the onset of high tide.
• **Conclusions:** Overall, the present study suggests this tidally driven oxygen pump as an explanation for commonly observed natural patterns in salt marsh recruitment near drainage channels and atop raised sediment mounds and reveals a promising way forward to promote the establishment of pioneers in the field.

Keywords: Micro-topography, salt marshes, establishment, restoration, drainage, oxygen penetration, *Salicornia procumbens*.

INTRODUCTION

Today, the rapidly growing human impact on natural systems is increasingly infringing upon and degrading the functioning and total area of ecosystems globally (Lotze *et al.*, 2006). The capacity for pioneer species to recolonize de-vegetated landscapes is central to reversing the process of degradation and the loss of their environmental services (Zhu *et al.*, 2019). However, the time scale over which re-colonization occurs varies dramatically between ecosystems. Amongst the most challenging environments for re-colonization are the biogeomorphic ecosystems: those that are controlled by dynamic physical forces that continuously restructure the environment by the erosion, transport and redistribution of sediment (Mullan and Bertness, 2006; Bayraktarov *et al.*, 2015). In such systems, the intensity of physical disturbances is mediated by the autogenic ecosystem engineering effects of vegetation, which stabilize the landscape. Clear examples of these systems involve coastal vegetation such as salt marshes, mangrove forests, seagrass meadows and biogenic dunes. The physically driven nature of biogeomorphic systems has also made them the most expensive and failure-prone targets for restoration (Suding *et al.*, 2004; Han *et al.*, 2015; Moffett *et al.*, 2015). At the core of this problem is a chicken-and-egg paradox wherein the removal of environmental infrastructure generated by ecosystem engineers makes the dynamic unmodified system nearly uninhabitable to the foundational organisms that lead to their development and stabilization (Corenblit *et al.*, 2011; Balke *et al.*, 2014).

Pioneering salt marsh vegetation is known to develop its own infrastructure to enhance drainage in order to terrestrialize harsh marine environments (Temmerman *et al.*, 2007; Kearney and Fagherazzi, 2016; Schwarz *et al.*, 2018). Salt marshes passively generate and benefit from space-filling networks of drainage channels that accelerate the drainage of the marsh platform (Xin *et al.*, 2011; Wilson *et al.*, 2014). Further physiological adaptions such as the development of aerenchyma common in major pioneer marsh species such as the genus *Spartina* also function to alleviate the biogeochemical stress in waterlogged sediments (Burdick, 1989; Maricle and Lee, 2002; Koop-Jakobsen and Wenzhöfer, 2015; Strain *et al.*, 2017). The inundated soils that typify the wetland environment experience a reduction in the available oxygen in the root layer due to the poor diffusion rate of oxygen into sediment whose interstitial spaces are occupied by water (Rabouille *et al.*, 2003; Marani *et al.*, 2006). Both the injection of oxygen into marine sediments by aerenchyma, and the recirculation of porewater imposed by marsh-induced drainage channels function to alleviate multiple stressors present in marine sediments. These stressors include a reduction in the available metabolic oxygen in the root layer (Howes and Teal, 1994; Maricle and Lee, 2007) and the build-up of toxic sulphide caused by microbial breakdown of organic matter in anoxic saline conditions (Linthurst and Seneca, 1980; Lamers *et al.*, 2013). However, these facilitative mechanisms require time to develop on their own (e.g. see Bouma *et al.*, 2009), and are not available during the critical early stages of pioneer development.

In the absence of these stress-mitigating functions, early-stage, establishing pioneer recruits may be required to take advantage of specific circumstances in the physical environment in order to maintain oxygen levels in the rhizosphere. Recruits, for instance, tend to appear in proximity to mounds generated by the fibrous algal group *Vaucheria* (R. van der Vijsel, NIOZ, Yerseke, the Netherlands, unpubl. res.; Fig. 1A) and tidal drainage channels formed either through physical or other biophysical feedbacks (Fig. 1B, C). They also appear atop raised micro-topography commonly generated and maintained by diatom biofilms (Blanchard *et al.*, 2000; Weerman *et al.*, 2010), or within artificial structures (Fig. 1D). Anecdotal evidence from haphazard observations suggests that salt marsh recruits grow at a faster rate and establish

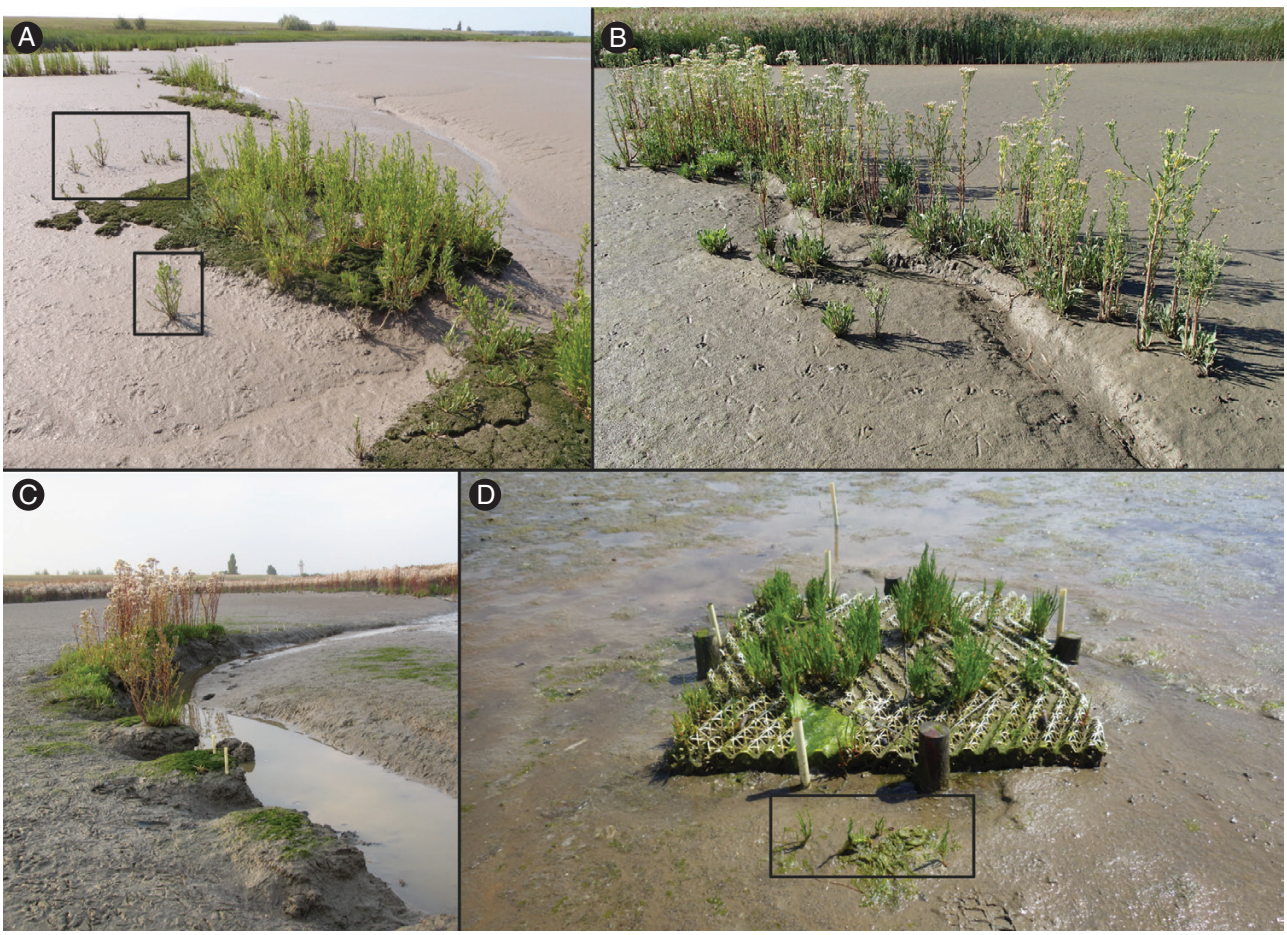

FIG. 1. Panel of anecdotal observations of salt marsh recruits: *Aster tripolium* in the Western Schelt estuary (A, B, C) and *Salicornia* spp. on the barrier island of Texel (D). Panel D features an artificially created sediment mound created for restoration purposes over which the natural establishment of *Salicornia* is visible. In the foreground of the image are natural recruits that have established on the adjacent tidal flat, which are much smaller than those found atop the artificial sediment mound. Recruits appear larger and at higher density on raised micro-topography deriving from hummock-forming biophysical feedbacks, or creek incision (see stunted growth within black rectangles in panels A and D). Panels A and B: photos by Jim van Belzen; panel C: photo by Roeland van de Vijsel; panel D: photo by Greg Fivash.

at higher densities within these specific environments (Fig. 1, see stunted growth within black rectangles). While the biogeochemical and biogeomorphic growth feedbacks between pioneer salt marsh development and the physical restructuring of their environment has been well studied (Chalmers, 1982; Bertness and Leonard, 1997; Bruno and Kennedy, 2000; Bouma *et al*., 2009, 2013), it remains unclear to what extent successful colonization by plant seedlings depends on specific soil drainage conditions. For example, drainage in relation to micro-topography is a concept absent from a recent review of establishment in coastal wetlands (see Friess *et al.*, 2012).

We hypothesize that elevated sediment surfaces in the mudflat topography promote growth of recruits by enhancing local drainage, which in turn stimulates sediment oxygenation. Enhanced growth should in turn be responsible for greater resistance to disturbance and the perceived correlation between establishment and such raised surfaces (Balke *et al.*, 2011; Hu *et al.*, 2015). Past field experiments on the relationship between salt marsh recruitment and sediment micro-topography have suggested that these surface structures benefit recruitment through the modification of soil moisture conditions, and thereby alter oxygen penetration below ground (Xin *et al.*, 2011; Lawrence *et al.*, 2018; Xie *et al.*, 2018; Mossman *et al.*, 2019). Yet to date no *in situ* measurements of the oxygen levels within these structures have been reported in the literature, and discussion of the driving factors behind the enhanced recruitment has remained speculative.

In this study, we determine to what extent elevated sediment surfaces drive the growth rate of seedlings of the model salt marsh pioneer *Salicornia procumbens*. This primary effect is contrasted against changes in above-ground inundation duration and the capacity for drainage to occur vertically through the sediment column. This is done through a mesocosm study in which sediment bed forms of various shapes are moulded to create conditions of contrasting potential for shallow lateral drainage, and thereby serve as substrate for salt marsh recruits. We then explore how soil moisture levels relate to soil oxygenation through a series of physical experiments, including a planar optode study wherein direct measurements of soil oxygen are made. This study represents a first step in the exploration of how and why sediment micro-topography effects the growth rate of recruiting salt marsh pioneers, and thereby provide new insights on how to provoke the establishment of salt marsh recruits in restoration applications.

MATERIALS AND METHODS

Species information

The model species featured in this study, *S. procumbens*, is a prolific annual species distributed widely over European marshes. It colonizes the tidal flat, despite having poorly developed aerenchyma with which to alleviate the anoxia within inundated sediments. It commonly appears in the lowest reaches of the pioneer zone and can be found over a wide salinity range, easily tolerating ocean salinity while also appearing at brackish estuarine marsh sites where salinity is highly variable (Davy *et al.*, 2001).

Growth effects of inundation duration, soil drainage and micro-topography (Experiment 1)

A mesocosm experiment was designed, which separated the interactions between independent features of tidal inundation: (1) the duration of above-ground inundation, (2) the capacity for the sediment to drain vertically during low tide, and (3) the effects of local sediment surface heterogeneity on these processes. By growing *S. procumbens* under each of these varying conditions in a full-factorial experiment it was possible to quantify to what extent each of these factors contributed to growth.

The experiment was performed in a climate chamber under controlled light and temperature settings (20 °C and 100 µmol photons m^{-2} s^{-1}), in three tanks that simulated twice-daily tidal inundation. Each tank was set to a different period of inundation: remaining inundated for 20, 35 and 50 % of the 12-h cycle, respectively. This set of inundation regimes was chosen to represent the full spectrum conditions experienced in the pioneer zone: 20 % inundation duration is a common scenario for pioneer zones of intermediate hydrodynamic energy, while 50 % represents an extreme inundation scenario (Balke *et al.*, 2016; van Belzen *et al.*, 2017). These tanks were composed of two basins: a reservoir and an experimental chamber between which water could be interchanged via a pump to produce tidal cycles (for details see Cao *et al.*, 2018).

The reservoir tanks were filled with 10 ppt water made from a mixture of filtered estuarine water of 30 ppt from the Oosterschelde and fresh water from the tap. Salinity was kept to a consistent value by periodically adding fresh water throughout the experiment. Salinity conditions reflected a typical spring climate scenario in the pioneer zone of the salt marshes within the Westernschelde, which varies between 30 and 5 ppt in the Dutch regions of the estuary (van Damme *et al.*, 2005). Low-salinity events driven by terrestrial rainfall discharge to the estuary act as a seasonal trigger for germination, and are a common environmental setting for growth in early life (Ungar,, 1977).

For use as growing pots, 126 cylindrical PVC caps of 12.5 cm diameter and 4 cm height were filled with sediment collected from the mudflat at the pioneer zone of the salt marsh ‘de Schorren' on the barrier island of Texel in the Wadden Sea (53.123063, 4.900131), where *Salicornia* is known to occur. Grain size analysis (Mastersizer 2000, Malvern Panalytical Ltd, Malvern, UK) showed that this sediment, typical of the Dutch Wadden Sea, was relatively coarse with a median sediment grain size of 145.6 ± 1.1 µm (mean ± s.e., $n = 28$). The average silt content was 21.2 ± 0.3 %, and the organic carbon content was 0.50 ± 0.01 % as measured by an elemental analyser (Carlo Erba NA-1500, Thermo Scientific, Waltham, MA, USA). The sediment was defaunated by first inducing anoxia underneath sealed plastic sheeting then through freezing at −15 °C for 72 h. Vertical soil drainage conditions were created by cutting out the bottom of the growth pot and securing fine mesh fabric over the hole to limit sediment loss. Half of all pots did not undergo this procedure and were impermeable to water so that no physical drainage could occur below the rim of the pot.

Lastly, sediment surfaces were modified according to three archetypal scenarios: (1) ‘flat' sediment surfaces were left equal to the height of the rim of the growth pot at all points; (2) ‘raised' sediment surfaces were elevated into a rounded hump 2 cm above the rim of the pot at their maximal point; and (3) ‘lowered'

surfaces were carved into a sloping bowl, 2 cm below the rim at the lowest point. The sediment in both the raised and the lowered treatments were equal in height to the rim of the pot at the edges (Fig. 2). These adjustments in relative sediment elevation were moulded in order to align with sediment forms commonly generated by physical and biophysical feedbacks in the field (as described above, Fig. 1). Dividing 126 pots among three sediment shape treatments, two vertical drainage treatments and three inundation duration treatments produced a replicate number of 7.

A total of 350 seeds of *S. procumbens*, harvested from the salt marsh of Ratekaai in the Eastern Schelt estuary (51°26′12.3″N, 4°12′39.8″E), were added to each pot by pressing the seeds lightly into the sediment. As a consequence of this approach, some seed loss via resuspension occurred. At the conclusion of the experiment after 33 d of growth, the above-ground structures of the *Salicornia* recruits were extracted from the pots by clipping the stems at the sediment interface. These individuals were then photographed for size quantification via image analysis (elaboration to follow). Recruitment of the original 350 seeds ranged between 19.4 and 57.7 % (68 and 202 individuals per pot). Lowered sediment surfaces tended to experience greater recruit densities while raised surfaces experienced lesser (Supplementary Data Fig. S1). This introduced an unforeseen factor into our study: varying individual densities between pots, which had the potential to affect individual growth.

Growth effects of micro-topography: an individual-based study (Experiment 2)

Agricultural trials on *Salicornia* cultured in high-density plots have found little evidence of self-thinning in this species (Ellison, 1987). However, to ensure that our conclusions were robust despite this complication, we conducted a second smaller-scale growth trial in which single *S. procumbens* individuals were grown in individualized 5-cm^3 square pots. The individualized pots prevented individual density from acting as a confounding factor in this experiment. The growth of 48 *S. procumbens* individuals were monitored over a period of 160 d. In this case, the sediment topology was the only adjusted environmental parameter, again comparing (1) raised, (2) flat (3) and lowered sediment surface treatments. Sediment surfaces were raised and lowered only 1 cm above or below the rim of the square pot. The experiment was repeated within a single tidal tank set to an inundation duration of 50 % so as to inflict the lowest possible growth rate on our plants, induced by high inundation duration. Meanwhile we limited the effect of the sediment surfaces by allowing all pots to drain vertically, following the technique used in experiment 1. By using drained conditions in which the sediment surface modifications may be expected to be the least effective and hence growth differences most difficult to perceive, we intended to demonstrate the robust nature of the effect that these surfaces have on growth. In this case, the growth of each individual was monitored repeatedly using a non-destructive technique using standardized photographs (illustrated in Supplementary Data Fig. S2).

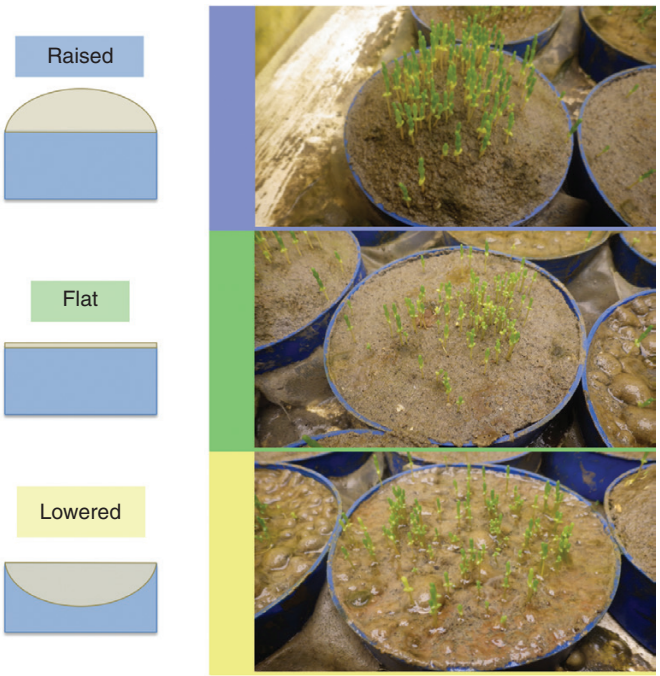

FIG. 2. The initial growth trial was performed in growth pots made from blue PVC caps, which are sealed containers that do not normally allow for any vertical drainage (unless modified). Each pot contained 350 individual *Salicornia procumbens* seeds. The three archetypal sediment topology treatments are shown.

Quantifying plant growth using photography (Experiments 1 and 2)

In both experiments, the measurement of plant size was performed using image analysis. Individual plants were placed against a high-contrast base-board and photographed alongside a scale. The planform area of each recruit was measured through analysis of these photographs using the software ImageJ. Each photo was converted into a binary image after setting hue, saturation and brightness thresholds (14 < Hue < 226, 0 < Saturation < 255, 0 < Brightness < 255) in order to properly differentiate the recruit from the base-board (Supplementary Data Fig. S3). In total, 126 individuals grown in a separate experiment to a range of sizes were analysed in this way before being dried at 60 °C for 48 h and weighed for stable dry biomass. A calibration curve was then generated to convert between individual recruit planform area and individual dry biomass for the remainder of the recruits. Not all plant species would be suitable for a conversion between planform area and mass because tissues could become obscured in photographs or appear at oblique angles. However, due to the cylindrical nature of *Salicornia*, which is a succulent plant with photosynthetic stems in place of leaves, this approach yielded an effective calibration (R^2 = 0.963, n = 126, P < 0.0001, Supplementary Data Fig. S4). With the photo technique, our capacity to measure small differences between individual size over a large number of individuals (17 393 individuals in this study) was greatly expanded. Furthermore, it allowed for accurate repeated measures of size to be performed un-invasively in the second growth experiment.

Quantifying the sediment water content (Experiment 1)

In order to measure the impact that various drainage/inundation regimes had on sediment water content at various depths,

we used a 2.5-cm-diameter open-ended cylindrical syringe to extract a sediment sample from each pot in the primary growth experiment ranging from the surface to the bottom of the pot. To measure sediment water content, the sample was then cut into 1-cm depth segments, weighed wet, dried at 60 °C to constant mass and weighed again. The sediment water content was calculated to be the proportional difference between these wet and dry mass measurements. Because differences in water content were constrained to the top 1 cm of the sediment column, analysis of water content differences between treatments ultimately considered only this top 1 cm.

Ground water drainage effects of micro-topography (Experiment 3)

In a third experiment, we measured changes in ground water level throughout the tidal cycle contrasted between different sediment surfaces. For these measurements to take place, PVC tubes (10 cm height, 12.5 cm diameter) were filled with sediment so the sediment surface was adjusted to be either 2 cm above or below, or equal to, the top edge of the PVC tube. These surfaces were then shaped to the elliptical bowl and hump dimensions seen in the growth experiment. To isolate the signal produced solely as a consequence of variation in the sediment surface, the pots were sealed to prevent vertical drainage. This sediment was then subjected to a tidal regime in which the sediment was saturated with water during a high tide period of 3 h and allowed to drain for a period of 9 h thereafter. For each sediment shape, we replicated ground water measurements in two separate PVC tubes. We did not attempt to distinguish between (or control for) the contribution of ground water loss specifically from evaporation or surface drainage between treatments. Rather, we were interested in how the variation in sediment surfaces would affect the ground water level, because both mechanisms would typically co-occur in the field.

To measure the drop in ground water level, photo measurements were made in time series over the low tide period. Within the centre of the sediment-filled PVC tubes, a 2.5-cm-diameter filter PVC tube surrounded in cloth mesh was installed so that the ground water could flow between this central region and the sediment. Measuring sticks were placed within this tube for scale. Photographs of the ground water level were taken in 5-min intervals for five tidal cycles. The ground water level was determined with respect to the height of the sediment surface. Photo analysis was performed in ImageJ. The accuracy of these measurements was limited by the size of one pixel, which in this case was ~0.02 mm.

Tidally driven oxygenation: sediment aeration effects of micro-topography (Experiment 4)

To measure sediment oxygenation, we performed a planar optode study comparing various sediment surfaces (described in Larsen *et al.*, 2011). The PVC tubes found in the ground water drainage experiments were cut in half, and the open sediment section was then pressed up against a pane of plexiglass to which the sensor foil (SF-RPSU4, PreSens - Precision Sensing GmbH, Regensburg, Germany) had been adhered. All sediment tubes were perforated at the base to allow drainage vertically. The use of this most pronounced aeration scenario ensured that the effects of the sediment topology on aeration were robust. The plexiglass and the pot were housed within a miniature tidal tank in which the inundation of 10 ppt seawater occurred for 3 h every 12 h. Humidity and temperature within the experimental area were controlled to remain constant at 100 % (to protect the foil) and 18 °C. Tidal periods were recorded using a Sensus-Ultra pressure logger. Three pots, one of each sediment shape, were placed within this chamber for a period of 48 h.

A VisiSens TD camera system (PreSens - Precision Sensing) captured the oxygen saturation (%) in the sediment over a 7 × 7-cm area as a series of jpeg-images taken once every 2 min (or once every 5 min in the case of the flat sediment treatment). These images were then converted into greyscale using the R library 'imager' (Barthelme, 2018). From this greyscale image, a 455 × 590-pixel area (6.24 cm depth range) was extracted to remove noise near the margins, where some degradation of the foil occurred. Every pixel row in the image, representing a depth interval of 0.01 cm, was averaged to produce a single mean oxygen saturation value at each depth, yielding a single oxygen profile for each snap-shot in the time series (Supplementary Data Fig. S5). All measurements were calibrated using a two-point calibration between oxygen-saturated and anoxic conditions, achieved by pumping either oxygen or nitrogen gas into the tidal chamber to saturation (0 % = 2.2082 internal ratio-units, 100 % = 1.2851 internal ratio-units; for technical details see manual of PreSens - Precision Sensing).

In order to characterize strong apparent changes in these profiles that occurred cyclically over the tidal cycle, we used a novel approach to analyse the profiles through time. Using the R library 'inflection' (Christopoulos, 2017), the inflection point of the profile curve was approximated for each image. Data below this inflection point were fitted to an exponential decay function. Based on the negative slope of this regression, the 'decline rate' of soil oxygen availability at depth could be parameterized and compared between sediment shape treatments. Because the planar optode becomes unreliable at near zero values, we fitted the linear regression using only oxygen saturation measurements located between the inflection point and the region up to 40 mm below it. This procedure produced a time series of values representing the rate of oxygen reduction at depth in the sediment over the tidal cycle, allowing us to easily visualize episodic oxygenation processes throughout the tidal cycle.

To quantify this periodic phenomenon for statistical analysis, the time series of 'oxygen decline rate' values was deconstructed into three characteristic components. Each tidal cycle for each sediment pot was taken as an experimental replicate. First, (1) during the equilibrium period of low tide between hour 6 and 12 of the 12-h tidal cycle, the decline rate values were averaged to estimate the level of oxygenation during low tide (Supplementary Data Fig. S6i). Second, (2) the decline rate value during peak oxygenation was measured in each tidal cycle (Fig. S6ii). Lastly, (3) the duration of each oxygenation event was measured by calculating the length of time between the onset of high tide and the moment that the oxygen decline rate returned to a value below 4.2 O_2 sat.% cm^{-2} (an arbitrary threshold set slightly below oxygen equilibrium, Fig. S6iii).

Statistical analyses

In experiment 1, average size within each pot was compared between treatment groups after log transformation of the data, due to the log-normal distribution of individual sizes within each pot. This yielded a set of 126 values that could be compared using a three-way ANOVA followed by 'Tukey honest significant difference' post-hoc pairwise comparisons of each factor (Table 1). In experiment 2, the growth rate of individuals was followed through time. At any given time point, the biomass of all individuals again formed a log-normal distribution. The growth of each individual through time was fitted with a power law function. This was the most parsimonious fit between regressions employing linear, exponential, Gompertz (sigmoid) function and power law functions. Model comparison was performed using Akaike's information criterion (AIC) (Akaike, 1969). An independent fit was made for each individual in the experiment, to produce a population of 'growth rates' (the exponent of the power law), which were compared in a one-way ANOVA between treatments. The log-transformed biomass of each individual at the conclusion of the experiment was also compared between treatments using the ANOVA method.

Data on the sediment water content satisfied assumptions of normality and heterogeneity of variance, permitting comparisons between treatments to be made using three-way ANOVA tests, as seen earlier in the primary growth experiment. Changes in ground water level between sediment pots over the low tide interval were analysed with regressions fit to either linear or exponential decay functions based on AIC model comparison. The time series of 'oxygen decline rate' values was deconstructed into three characteristic components (as described above, Supplementary Data Fig. S6) on which one-way ANOVA was performed to compare the effects of sediment shape treatments on oxygenation processes. All analyses were performed in R version 3.6.0 (R Core Development Team, 2008).

RESULTS

Growth effects of inundation duration, soil drainage and micro-topography (Experiment 1)

In our primary growth experiment, we found that all treatment groups had a statistically detectable effect on growth. However, increasing the height of the sediment surface by 2 cm relative to the rim of the growth pot made a much larger positive contribution to growth than did reducing the inundation duration or allowing vertical drainage (Fig. 3; Table 1). Inundation duration alone played a marginal role in effecting growth rates ($F_{1,108}$ = 4.05, n = 42, P = 0.020), despite fairly dramatic variation in tidal regimes (ranging from 20 to 50 %): The contribution to growth from manipulating above-ground inundation was only statistically perceptible in post-hoc tests between the most extreme treatment differences (P = 0.016, n = 42). Reducing the inundation duration from 50 to 20 % increased the average harvest biomass by only 12.6 ± 8.0 % (mean ± s.e.). A similar 12.5 ± 6.6 % increase in harvest biomass could be found in pots that drained vertically ($F_{1,108}$ = 11.63, n = 63, P < 0.001). Meanwhile, raised sediment surfaces increased harvest biomass by 26.5 ± 7.6 % against flat surfaces (P < 0.0001, n = 42), and by 37.1 ± 7.9 % against hollow surfaces (P < 0.0001, n = 42). This represented an effect between two and three times greater in magnitude than that of the other factors in the experiment. The quantitative differences in average harvest biomass between flat and hollow sediment shapes, by contrast, were not statistically significant (P = 0.162, n = 42), a size difference of 8.4 ± 8.9 %.

The effect of the raised surfaces was notably reduced in the tank performing the intermediate inundation duration treatment. The percentage difference in individual size between raised and lowered surface treatments in the 35 % inundation duration tank was 9.8 ± 8.1 % against a difference of 53.3 ± 7.8 % found in the other two tidal tanks. This reduced performance is indicated in the fit of our ANOVA model as a U-shaped interaction between the effect of sediment shape under varying inundation duration (Table 1). This treatment effect was not distinguishable from a random effect of the tank, because inundation regimes were not replicated between multiple tanks. Furthermore, a weakly significant three-way interaction between all factors in our experiment also appeared in our ANOVA model (Table 1).

Growth effects of micro-topography: an individual-based study (Experiment 2)

ANOVA tests showed that growth rate varied as a consequence of sediment surface treatments ($F_{2,45}$ = 33.73, n = 16, P < 0.001, Fig. 4). Post-hoc comparison of individual growth rates between treatments strongly distinguished between raised sediment beds and the other treatments (P < 0.001, n = 16 in both cases) whereas it did not detect differences in growth in individuals growing on flat and lowered sediment beds (P = 0.970, n = 16). Individual recruit growth rates were on

TABLE 1. *Analysis of variance table for the three-way ANOVA performed on the initial growth trial. This test distinguishes the relevance of the various environmental parameters on the mean biomass of* Salicornia procumbens *recruits after the ~1-month early-life growing period. Biomass values were log-transformed to suit the assumption of normality.*

	d.f.	Sum of squares	Mean square	F-value	P-value
Sediment shape	2	2.261	1.130	30.175	3.886×10^{-11}
Vertical drainage capacity	1	0.436	0.436	11.633	0.001
Inundation duration	2	0.303	0.152	4.047	0.020
Sediment shape: vertical drainage capacity	2	0.129	0.065	1.726	0.183
Sediment shape: inundation duration	4	0.604	0.151	4.028	0.004
Vertical drainage capacity: inundation duration	2	0.108	0.054	1.439	0.242
Sediment shape: vertical drainage capacity: inundation duration	4	0.440	0.110	2.938	0.024
Residuals	108	4.61	0.040		

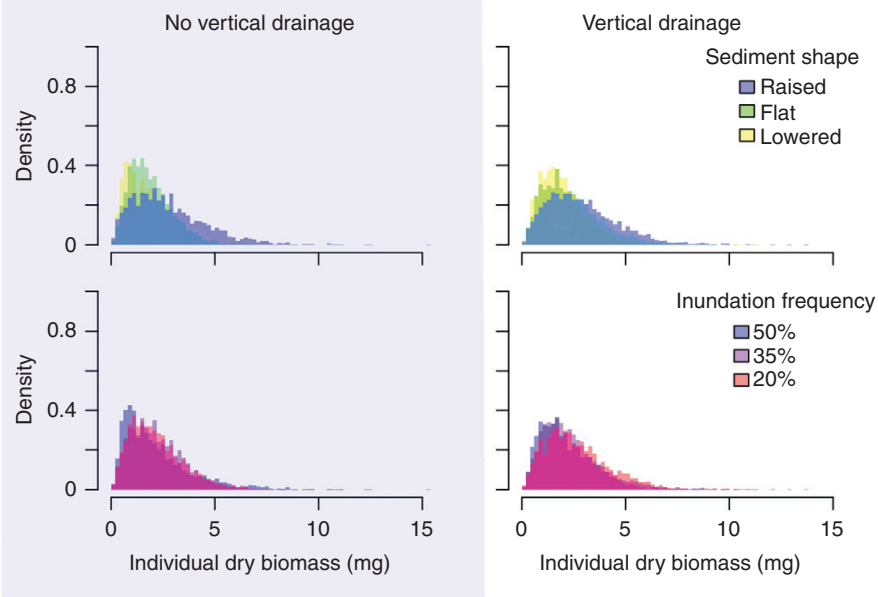

FIG. 3. Probability density plots displaying the distribution of *Salicornia procumbens* individual sizes (dry biomass in mg) found between the treatments in the experiment. Individual biomass follows a log-normal distribution in all cases. In the top right and left frame, we contrast the effects of the sediment topology treatments on the growth of recruits. In the lower right and left frames, the effect of inundation duration on growth is displayed. The capacity of the sediment to drain vertically splits the groups from left to right (figures within the blue box cannot drain vertically). Clear treatment effects of sediment topology are visible, representing an average increase in average size of 20–30 % in raised sediment surfaces (Table 1, $P < 0.001$, $n = 42$). By contrast, there are only minute effects of inundation duration on the growth of recruits ($P < 0.027$, $n = 42$).

average 24.9 ± 1.4 % higher on raised surfaces when compared to other groups. After 160 d, individuals growing on 1-cm-high raised sediment mounds were on average 39.4 ± 0.4 % larger than the remaining population in the experiment ($P < 0.001$, $n = 16$). Those individuals growing in flat sediment and in 1-cm lowered depressions remained indistinguishable ($P = 0.964$, $n = 16$).

Sediment water content (Experiment 1)

To outline the mechanistic link between sediment topology and enhanced growth, we measured both the sediment water content of the sediments in the initial growth experiment (experiment 1) at the experimental harvest, and changes in the ground water level within the contrasting sediment surfaces in a separate experiment. In general, water content varied only in the top 1 cm of the sediment column where it was on average wetter than what was found further at depth (Supplementary Data Fig. S7). While water content did differ between sediment surfaces ($F_{2,114} = 120.95$, $n = 42$, $P < 0.0001$), significant changes were not detectable between raised sediments against their flat counterparts ($P = 0.144$, $n = 42$). Instead, the strongest differences appeared in lowered pots (Supplementary Data Fig. S8). Here, water content in the top 1 cm increased from 26.8 ± 0.2 % in flat and raised sediments to 36.2 ± 1.0 % in lowered sediments ($P < 0.0001$, $n = 42$, in both cases). Direct vertical soil drainage had a smaller effect on sediment water content ($F_{1,43} = 6.39$, $n = 63$, $P = 0.015$), decreasing it by 0.7 ± 0.6 % water content where drainage was possible. In contrast, variation in inundation duration alone had no measurable effect ($F_{1,114} = 0.55$, $P = 0.459$, $n = 42$).

Ground water drainage effects of micro-topography (Experiment 3)

We found that the ground water in raised sediment surfaces above the rim of the pot rapidly drained away after the onset of the low tide interval, while sediment within the PVC tubes and in the pooling surface water over the hollows displayed a more gradual rate of water loss driven by evaporation (Fig. 5). In raised sediment, the ground water depth decreased by approximately three times as much over the low tide period as seen in non-draining flat surfaces, a difference in this experiment of 1.23 ± 0.01 cm. In lowered sediment surfaces, pooling surface water remained permanently over the sediment at a water depth fluctuating between 2 and 1.76 cm over the low tide interval.

Tidally driven oxygenation: sediment aeration effects of micro-topography (Experiment 4)

Oxygen measurements taken using the planar optode showed constant above-ground oxygen saturation during both low and high tide. Below ground, we detected an exponential decline in oxygen saturation at increasing depth in the sediment, typical for a sediment oxygen profile (conceptual overview in Fig. 6A). This stable profile was disturbed cyclically at the onset of high tide and returned to its initial state after a period of minutes to hours (visualized in Fig. 7, and also in video format in Supplementary data Fig. S9A–C). The intensity and duration of these events varied between treatments (Fig. S6).

The stable low tide oxygen profile [measured by the rate of decrease in oxygen saturation at depth (O_2 sat.% cm^{-2})] varied subtly between sediment surface types [$F_{2,12} = 4.51$, $n = (4,$

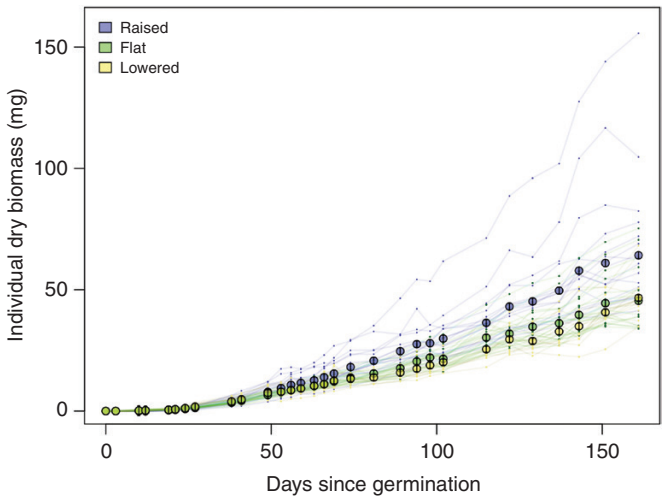

FIG. 4. The growth of *Salicornia procumbens* individuals is shown over the 162-d experimental period. Large circles show the median size for each treatment group at each measuring date, while the small coloured points display the data values for each individual. The highly inflated values above the median suggest a log-normally distributed population. Individuals growing on 1-cm-tall raised sediment platforms that can drain laterally grow to be on average 38.8 % larger than individuals in the other treatment groups by the end of the experiment ($P < 0.001$, $n = 16$). Comparisons between treatments groups were performed both through regression analysis of the time series and through pairwise comparisons between the treatment groups at each time step (details in the text).

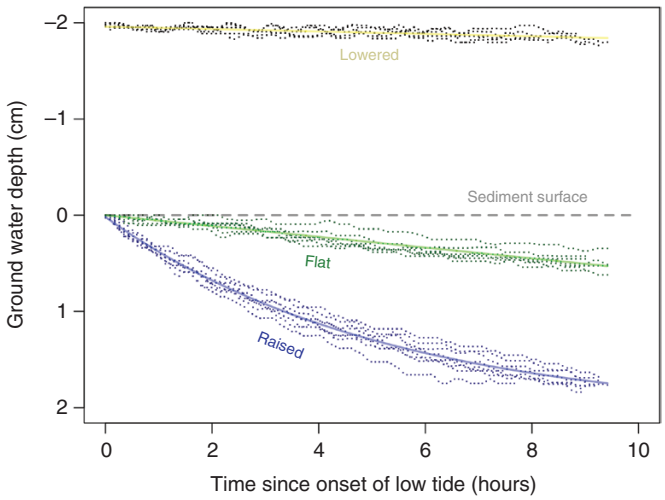

FIG. 5. Change in ground water level within or pooling above three sediment surface treatments across the low tide interval. Points represent measured values from five repeated tidal cycles, while the coloured regression lines show predicted values for each treatment group. Raised surfaces that are able to drain laterally decrease in ground water level most strongly (shown in blue), yet evaporation within the sediment also plays an important role in decreasing ground water level (best displayed in flat sediment, in green).

7, 4), $P = 0.035$]. Distinctions between contrast groups were only statistically detectable between the extremes: raised and lowered sediment shapes ($n = 4$, $P = 0.036$). Trends across groups were consistent, however, wherein raised sediments had the greatest oxygen penetration (rate: 4.33 ± 0.27), followed by flat (rate: 4.75 ± 0.05) and then lowered surfaces (4.92 ± 0.05). Here, low oxygen decline rate values correspond to greater oxygen penetration (Supplementary Data Fig. S6i).

Accompanying these subtle differences in oxygen profiles, we observed episodic oxygenation events that occurred at the onset of high tide, wherein oxygen saturation reached high levels in deep layers of the sediment (Fig. 7). During the most extreme oxygenation events the oxygen-saturated zone exceeded the maximum measurable depth of our sensor foil, 4 cm below the sediment surface. The duration of the period of high oxygen availability was considerably greater in raised sediment surfaces than in other treatments [Supplementary Data Fig. S6iii, $F_{2,13} = 11.91$, $n = (4, 7, 4)$, $P = 0.001$]. The available sediment oxygen returned to an equilibrium state (defined by passing the threshold decline rate of 4.2 O_2 sat.% cm^{-2}) in lowered and flat sediments after ~0.5 ± 0.3 h (lowered) and 1.3 ± 0.3 h (flat). In contrast, the same process required on average 3.6 ± 0.7 h in the raised sediment bed. The peak depth of oxygen penetration during these events also differed between sediment surfaces [Fig. S6ii, $F_{2,13} = 4.33$, $n = (4, 7, 4)$, $P = 0.036$]. The oxygen decline rate reached an average minimum value of 1.15 ± 0.42 (raised), 2.73 ± 0.46 (flat) and 3.51 ± 0.63 (lowered) O_2 sat.% cm^{-2} during these events.

DISCUSSION

Our experiments clearly demonstrate the major role that raised sediment micro-topography can play in the determination of the growth rate of *S. procumbens*. In both of our growth trials (experiments 1 and 2), there was a consistent trend toward increased growth on raised surfaces. Manipulations of sediment surface shapes were furthermore shown to have specific consequences for sediment drainage and oxygenation. Raised sediment surfaces allow for fast ground water drainage over the low tide interval as well as subtly modifying the equilibrium oxygen state to be more oxygen-rich at depth. At high tide, raised surfaces increased both the depth and the duration of episodic tidally driven oxygenation events. These results together provide substantial but indirect support that elevated micro-topography boosts growth of *S. procumbens* through these oxygenating mechanisms. The present findings furthermore have major implications for both understanding the natural recruitment process and, as discussed below, unlock a novel way to improve current restoration practices.

Answers and questions on the mechanisms by which micro-topography enhances plant growth

Our expectation was that sediment would become better aerated as a direct consequence of drier sediment conditions during the low tide interval, measurable in changes to either the ground water level or water content of the sediment. This causal link would have been supported by measurements that showed either (1) variation in the equilibrium oxygen profile between contrasting sediment surfaces or (2) variation in this equilibrium state over the low tide period within treatments. Such conclusions could not be supported by our results, however. Raised sediment surfaces marginally increased soil aeration during low tide (Fig. 6B), but this did not follow logically from concurrent differences in (1) soil moisture, which did not differ between flat and raised surfaces. Furthermore, (2) the oxygen profile of all sediment shapes remained stable over the

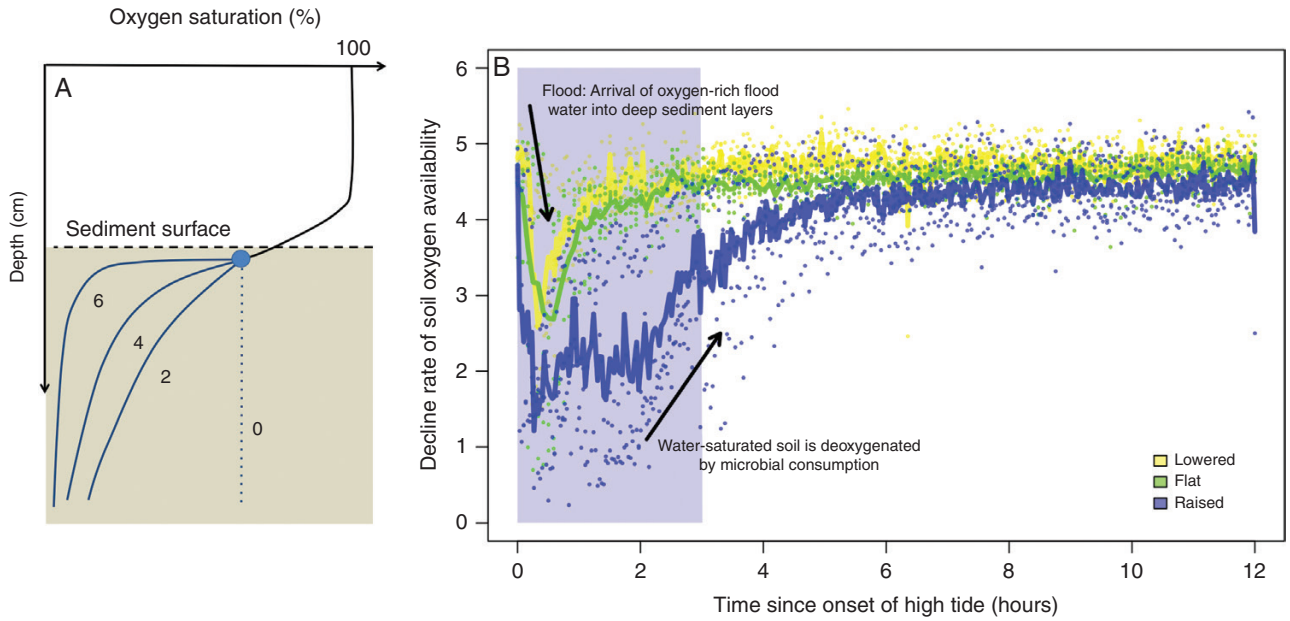

FIG. 6. (A) Conceptual diagram of three contrasting examples of oxygen profiles expressing different extents of oxygen availability in the sediment throughout the tidal cycle. The method used to capture the variation in oxygen through time uses the 'rate' parameter of the exponential decay function (coloured line) fitted to the data points below the inflection point of the profile. (B) Fluctuations in the 'decline rate' of oxygen availability (rate parameter) over the tidal cycle. The thick line represents a moving average between the points displayed in colours indicating the sediment topology. Enhanced oxygenation at high tide suggests that the initial flood forces oxygenated water into the sediment. This tidal oxygen pump is exaggerated in raised sediment surfaces (blue), probably due to enhanced drainage during the low tide interval.

low tide period whilst significant changes in ground water level took place (Fig. 5). Instead, our results support an altogether different explanation for the observed enhanced oxygenation of raised sediment surfaces.

We found that the equilibrium state of oxygen penetration was perturbed by an episodic event of massive oxygenation that occurred synchronously with the onset of high tide. Furthermore, the magnitude of the oxygenation event was exaggerated in raised sediment surfaces (Fig. 7). Our explanation of this phenomenon involves a tidally driven porewater recirculation process. Herein, the arrival of oxygen-rich flood waters causes the relatively denser water to displace the deoxygenated gas present in sediment pore spaces. A similar process has been described in field studies on porewater flow dynamics at a regional scale over the mudflat shelf (Røy *et al.*, 2008; Jansen *et al.*, 2009). In this case, the oxygenation of the sediment occurred primarily during high tide as a consequence of hydrodynamic forcing by waves. The extent of oxygenation in elevated sediment surfaces may be related to the capacity for the sediment to drain during low tide, because as water is replaced with gas in the pores during soil drainage, it increases the pore volume that is available to circulation by flood waters. However, a full understanding of how this process functions in relation to sediment micro-topography and ground water level remains incomplete. The physical structure of the raised sediment surface may also play a role in amplifying recirculation. This is suggested by the evidence that vertical drainage in the sediment column alone (as seen in the flat sediment core in the planar optode experiment) seems to have minimal effect on recirculation despite having a considerable effect on the ground water level.

Plant growth analyses on micro-topography: strengths, limitations and future questions

How marsh species adapt to withstand soil anoxia in inundated sediments has been the focus of many past studies (Pezeshki, 2001, and references therein). Pioneering salt marsh species are known to flexibly modify their root architecture and biomass allocation as a consequence of soil drainage, as measured in adult plants (Justin and Armstrong, 1987; Padgett *et al.*, 1998; Bouma *et al.*, 2001*a*, *b*). This is thought to reduce the physiological damage and growth inhibition caused by the intrusion of roots into the anoxic zone (Mendelssohn, 1981; Kozlowski, 1984; Koch and Mendelssohn, 1989; Lamers *et al.*, 2013). The below-ground processes that have been the focus of this study are likely to have had an impact on below-ground plant structures. For instance, tidal dynamics that force oxygen into deeper sediment layers through hydrodynamic forcing have been demonstrated to maintain reduced sulphide concentrations in the sediment (Røy *et al.*, 2008; Jansen *et al.*, 2009). Such an effect in our experiment would probably have led to greater root penetration wherever sulphide concentrations were suppressed by porewater recirculation. Thus, measurements of modifications in the root architecture between plants growing on and off raised sediment surfaces would give further support to our claim that the amplified tidal porewater re-circulation of these surfaces is relevant to plant growth.

However, at no point in this study was the below-ground biomass or root structure of the recruits measured. In both growth experiments (experiments 1 and 2), the inability to measure below-ground biomass resulted from trade-offs in experimental design. In experiment 1, we opted to grow plants together in shared pots in order to reduce the strong noise caused

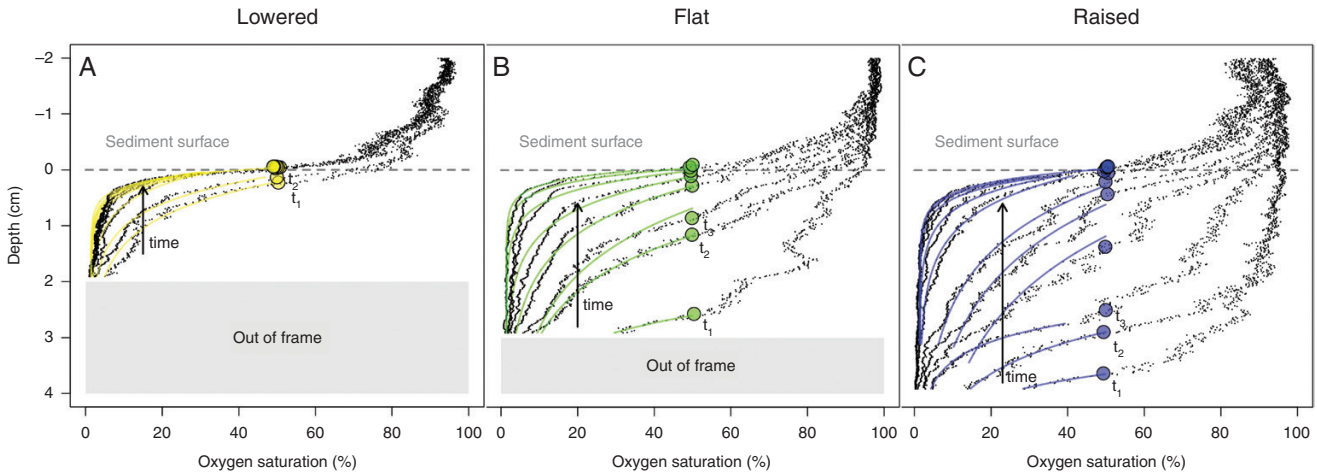

FIG. 7. A series of oxygen profiles are divided between the three sediment topology treatments in the three separate panels: raised (A), flat (B) and lowered (C). Oxygen profiles change drastically at the onset of high tide, represented by the lower-rightmost profile, and then return to an equilibrium state typified by the upper-leftmost profile in each panel. Comparison of the panels shows the exaggeration of the oxygenation event that is a consequence of sediment topology. Coloured lines indicate an exponential decay regression fit for each profile, which was used to draw the time series seen in Fig. 4 (details in the text). Due to constraints on the experimental set-up, raised sediment filled a greater region of the sampling frame so that those profiles could therefore be measured to greater depth. Differences in sampling range are represented by the grey rectangle.

by individual variability, while taking care to use experimental resources efficiently. At the same time, it made it impossible to distinguish individual roots within the entangled root mat. Because ultimately a different number of individuals developed in each pot, measurements of bulk root biomass between treatment groups were not meaningful. In the second growth trial, the photo time series method allowed us to un-invasively measure the change in individual plant size over time. This allowed us to explore the effect of sediment surfaces on the growth rate, which was a major strength of the study. Yet it was unable to track below-ground growth. This has left unanswered questions pertaining to below-ground root-growth processes on raised sediment surfaces, a topic that will no doubt bear fruitful insights in future research.

Implications from current work for coastal management and marsh restoration

This study demonstrates that surface topology has an overriding effect on the growth rate of young pioneer seedlings and thus contributes to a more complete understanding of how pioneering vegetation manages to colonize unmodified habitat. Hence, it also presents a potentially promising mechanism by which salt marsh growth rates can be accelerated in a field setting in order to enhance restoration success. Recruits that are establishing in disturbance-driven biogeomorphic landscapes require time to develop their defences and restructure their environments into stable and habitable zones (Bouma *et al.*, 2009; Friess *et al.*, 2012). To facilitate the circumstances in which such establishment can occur, restoration projects may utilize elevation differences introduced by landscape heterogeneity on a local scale to replicate this growth effect in the field. This should reduce the required length of the disturbance-free 'window of opportunity' required for successful natural establishment, and increase the likelihood of establishment events to occur (Hu *et al.*, 2015).

In the case of salt marshes, there is in fact a historical precedent for invoking natural recruitment through the modification of soil drainage. Dating back to the 14th century in northern Europe, Frisians performed land reclamation to extend the agricultural area by digging drainage channels in the tidal flat (Beck and Airoldi, 2007; de Groot and van Duin, 2013). This technique, known as 'kwelderwerken', ultimately motivated the establishment of salt marshes over ditched areas. In the modern era, the act of ditch-digging using heavy machinery is an expensive and labour-intensive process on soft-sediment mudflats. Yet, there could be other means by which similar drainage conditions could be produced through more passive means. To date, money is often spent to level sites in large-scale mudflat restoration projects. Freedom in contract to have natural heterogeneity persist represents a win–win scenario that would both reduce costs and accelerate restoration (Lawrence *et al.*, 2018). Moreover, exaggerated elevational differences can be produced by mimicking the physical restructuring of the landscape generated by the above-ground structures of salt marsh pioneers, which enhance local sedimentation. This has been successfully performed before using bamboo poles (Bouma *et al.*, 2007) and biodegradable lattice structures (Fig. 1D). The essence of this approach could be replicated using many kinds of epibenthic structures. Such constructions have been shown to passively capture sediment to create raised circular hummocks, similar to those typical of expanding clonal salt marsh patches. Solutions, like this one, wherein naturally occurring physical forces are manifested to intentionality shape the environment, have the potential to be extremely cost-effective.

CONCLUSION

This study provides an example of how by manipulating the topology of the pioneer zone, the growth rate of the pioneer vegetation, here *Salicornia procumbens*, can be accelerated. This appears to be the consequence of a previously unreported phenomenon in which elevated micro-topography amplifies

tidally driven sediment oxygenation events. Taking advantage of this natural phenomenon could play a central role in reducing the required disturbance-free interval for natural recruitment in the field, and thereby increase the frequency at which natural recruitment should occur. Similar approaches, wherein natural establishment is facilitated by manipulating the potential for recruits to overcome size-dependent thresholds, may become widely applicable solutions to restoration problems in diverse biogeomorphic settings.

SUPPLEMENTARY DATA

Supplementary data are available online at https://academic.oup.com/aob and consist of the following. Fig. S1: The number of recruits per pot in the initial growth experiment at harvest for each sediment shape treatment. Fig. S2: Time series analysis of *S. procumbens* growth using photographs of individuals taken periodically. Fig. S3: *S. procumbens* recruits from the initial growth trial against a high-contrast red base board in preparation for photo quantification of the total above-ground planform area. Fig. S4: The calibration curve used to calculate *S. procumbens* above-ground dry biomass based on the platform area of individuals taken from photographs. Fig. S5: A snapshot of the image generated by the planar optode experiment. Fig. S6: Three characteristic oxygen signals over the tidal cycle and various methods for quantification of episodic oxygenation events, contrasted between sediment shape treatments. Fig. S7: Water content of the sediment used in the first growth trials at depth in the sediment. Fig. S8: Water content of the sediment used in the first growth trials against sediment topology treatments. Fig. S9: Video showing a time series of oxygen profiles demonstrating a typical oxygenation event between the three sediment topology treatments.

FUNDING

This work was supported by Nederlandse Organisatie voor Wetenschappelijk Onderzoek (NWO)/Toegepaste en Technische Wetenschappen (TTW)-Open Technologieprogramma (OTP) grant 14424, in collaboration with private and public partners: Natuurmonumenten, STOWA, Rijkswaterstaat, Van Oord, Bureau Waardenburg, Enexio and Rodenburg Biopolymers, and by the Vlaams-Nederlandse Schelde Commissie (VNSC) project 'Vegetation modeling HPP' [contract 3109 1805].

ACKNOWLEDGEMENTS

We thank Lennart van IJzerloo and Jeroen van Dalen for assistance with equipment and measuring apparatus as well as providing the seeds used in this study. We also thank Anton Tramper for his technical expertise in the use of the planar optode system and Bert Sinke and Arne den Toonder for supplying and maintaining the experimental facilities.

LITERATURE CITED

Akaike H. 1969. Fitting autoregressive models for prediction. *Annals of the Institute of Statistical Mathematics* **21**: 243–247.

Balke T, Bouma TJ, Horstman EM, Webb EL, Erftemeijer PLA, Herman PMJ. 2011. Windows of opportunity: thresholds to mangrove seedling establishment on tidal flats. *Marine Ecology Progress Series* **440**: 1–9.

Balke T, Herman PMJ, Bouma TJ. 2014. Critical transitions in disturbance-driven ecosystems: identifying windows of opportunity for recovery. *Journal of Ecology* **102**: 700–708.

Balke T, Stock M, Jensen K, Bouma TJ, Kleyer M. 2016. A global analysis of the seaward salt marsh extent: the importance of tidal range. *Water Resources Research* **52**: 3775–3786.

Barthelme S. 2018. imager: Image processing library based on 'CImg'. R package version 0.41.1. Available at: https://CRAN.R-project.org/package=imager.

Bayraktarov E, Saunders MI, Abdullah S, *et al.* 2015. The cost and feasibility of marine coastal restoration. *Ecological Applications* **26**: 1055–1074.

Beck M, Airoldi L. 2007. Loss, status and trends for coastal marine habitats of Europe. *Oceanography and Marine Biology* **45**: 345–405.

van Belzen J, van de Koppel J, Kirwan ML, *et al.* 2017. Vegetation recovery in tidal marshes reveals critical slowing down under increased inundation. *Nature Communcations* **8**: 15811. doi: 10.1038/ncomms15811.

Bertness MD, Leonard GH. 1997. The role of positive interactions in communities: lessons from intertidal habitats. *Ecology* **78**: 1976–1989.

Blanchard GF, Paterson DM, Stal LJ, *et al.* 2000. The effect of geomorphological structures on potential biostabilisation by microphytobenthos on intertidal mudflats. *Continental Shelf Research* **20**: 1243–1256.

Bouma TJ, Koutstaal B, van Dongen M, Nielsen KL. 2001*a*. Coping with low nutrient availability and inundation: root growth responses of three halophytic grass species from different elevations along a flooding gradient. *Oecologia* **126**: 472–481.

Bouma TJ, Nielsen KL, van Hal J, Koutstaal B. 2001*b*. Root system topology and diameter distribution of species from habitats differing in inundation frequency. *Functional Ecology* **15**: 360–369.

Bouma TJ, van Duren LA, Temmerman S, *et al.* 2007. Spatial flow and sedimentation patterns within patches of epibenthic structures: combining field, flume and modelling experiments. *Continental Shelf Research* **27**: 1020–1045.

Bouma TJ, Friedrichs M, van Wesenbeeck BK, Temmerman S, Graf G, Herman PMJ. 2009. Density-dependent linkage of scale-dependent feedbacks: a flume study on the intertidal macrophyte *Spartina anglica*. *Oikos* **118**: 260–268.

Bouma TJ, Temmerman S, van Duren LA, *et al.* 2013. Organism traits determine the strength of scale-dependent bio-geomorphic feedbacks: a flume study on three intertidal plant species. *Geomorphology* 180–181: 57–65.

Bruno JF, Kennedy CW. 2000. Patch-size dependent habitat modification and facilitation on New England cobble beaches by *Spartina alterniflora*. *Oecologia* **122**: 98–108.

Burdick DM. 1989. Root aerenchyma development in *Spartina patens* in response to flooding. *American Journal of Botany* **76**: 777–780.

Cao H, Zhu Z, Balke T, Zhang L, Bouma TJ. 2018. Effects of sediment disturbance regimes on *Spartina* seedling establishment: Implications for salt marsh creation and restoration. *Limnology and Oceanography* **63**: 647–659.

Chalmers AG. 1982. Soil dynamics and the productivity of *Spartina alterniflora*. In: Kennedy VS,ed. *Estuarine comparisons*. Gleneden Beach: Academic Press, 231–242.

Christopoulos DT. 2017. inflection: Finds the Inflection Point of a Curve. R package version 1.3. Available at: https:/CRAN.R-project.org/package=inflection.

Corenblit D, Baas ACW, Bornette G, *et al.* 2011. Feedbacks between geomorphology and biota controlling Earth surface processes and landforms: a review of foundation concepts and current understandings. *Earth-Science Reviews* **106**: 307–331.

van Damme S, Struyf E, Maris T, *et al.* 2005. Spatial and temporal patterns of water quality along the estuarine salinity gradient of the Scheldt estuary (Belgium and The Netherlands): results of an integrated monitoring approach. *Hydrobiologia* **540**: 29–45.

Davy AJ, Bishop G, Costa CS. 2001. Biological flora of the British Isles: *Salicornia*. *Journal of Ecology* **89**: 681–707.

Ellison AM. 1987. Density-dependent dynamics of *Salicornia europaea* monocultures. *Ecology* **68**: 737–741.

Friess DA, Krauss KW, Horstman EM, *et al.* 2012. Are all intertidal wetlands naturally created equal? Bottlenecks, thresholds and knowledge gaps to mangrove and saltmarsh ecosystems. *Biological Reviews* **87**: 346–366.

de Groot AV, van Duin WE. 2013. Best practices for creating new salt marshes in an estuarine setting, a literature study. In: *Rapport/IMARES Wageningen UR; No. C145/12*. Den Helder: IMARES, 1–39.

Han Q, Komatsu T, Cunha A, *et al.* 2015. Global analysis of seagrass restoration: the importance of large-scale planting. *Journal of Applied Ecology* **53**: 567–578.

Howes BL, Teal JM. 1994. Oxygen loss from *Spartina alterniflora* and its relationship to salt marsh oxygen balance. *Oecologia* **97**: 431–438.

Hu Z, van Belzen J, van Der Wal D, *et al.* 2015. Windows of opportunity for salt marsh vegetation establishment on bare tidal flats: the importance of temporal and spatial variability in hydrodynamic forcing. *Journal of Geophysical Research G: Biogeosciences* **120**: 1450–1469.

Jansen S, Walpersdorf E, Werner U, Billerbeck M, Böttcher ME, Beer D De. 2009. Functioning of intertidal flats inferred from temporal and spatial dynamics of O_2, H_2S and pH in their surface sediment. *Ocean Dynamics* **59**: 317–332.

Justin SHFW, Armstrong W. 1987. The anatomical characteristics of roots and plant response to soil flooding. *The New Phytologist* **106**: 465–495.

Kearney WS, Fagherazzi S. 2016. Salt marsh vegetation promotes efficient tidal channel networks. *Nature Communications* **7**: 12287 EP, doi: 10.1038/ncomms12287.

Koch MS, Mendelssohn IA. 1989. Sulphide as a soil phytotoxin: differential responses in two marsh species. *Journal of Ecology* **77**: 565–578.

Koop-Jakobsen K, Wenzhöfer F. 2015. The dynamics of plant-mediated sediment oxygenation in *Spartina anglica* rhizospheres—a planar optode study. *Estuaries and Coasts* **38**: 951–963.

Kozlowski TT. 1984. Plant responses to flooding of soil. *BioScience* **34**: 162–167.

Lamers LPM, Govers LL, Janssen ICJM, *et al.* 2013. Sulfide as a soil phytotoxin – a review. *Frontiers in Plant Science* **4**: 268.

Larsen M, Borisov SM, Grunwald B, Klimant I, Glud RN. 2011. A simple and inexpensive high resolution color ratiometric planar optode imaging approach: application to oxygen and pH sensing. *Limnology and Oceanography: Methods* **9**: 348–360.

Lawrence PJ, Smith GR, Sullivan MJP, Mossman HL. 2018. Restored saltmarshes lack the topographic diversity found in natural habitat. *Ecological Engineering* **115**: 58–66.

Linthurst RA, Seneca ED. 1980. The effects of standing water and drainage potential on the *Spartina alterniflora* – substrate complex in a North Carolina salt marsh. *Estuarine and Coastal Marine Science* **11**: 41–52.

Lotze HK, Lenihan HS, Bourque BJ, *et al.* 2006. Depletion degradation, and recovery potential of estuaries and coastal seas. *Science* **312**: 1806–1809.

Marani M, Silvestri S, Belluco E, *et al.* 2006. Spatial organization and ecohydrological interactions in oxygen-limited vegetation ecosystems. *Water Resources Research* **42**: W06D06, doi:10.1029/2005WR004582.

Maricle BR, Lee RW. 2002. Aerenchyma development and oxygen transport in the estuarine cordgrasses *Spartina alterniflora* and *S. anglica*. *Aquatic Botany* **74**: 109–120.

Maricle BR, Lee RW. 2007. Root respiration and oxygen flux in salt marsh grasses from different elevational zones. *Marine Biology* **151**: 413–423.

Mendelssohn IA, McKee KL, Patrick WH. 1981. Oxygen deficiency in *Spartina alterniflora* roots: metabolic adaptation to anoxia. *Science* **23**: 439–441.

Moffett KB, Nardin W, Silvestri S, Wang C, Temmerman S. 2015. Multiple stable states and catastrophic shifts in coastal wetlands: progress, challenges, and opportunities in validating theory using remote sensing and other methods. *Remote Sensing* **7**: 10184–10226.

Mossman HL, Grant A, Davy AJ. 2019. Manipulating saltmarsh microtopography modulates the effects of elevation on sediment redox potential and halophyte distribution. *Journal of Ecology* 1–13. doi: 10.1111/1365–2745.13229.

Mullan C, Bertness MD. 2006. Ecosystem engineering across environmental gradients: implications for conservation and management. *Biosciences* **56**: 211–218.

Padgett DE, Rogerson CB, Hackney CT. 1998. Effects of soil drainage on vertical distribution of subsurface tissues in the salt marsh macrophyte *Spartina alterniflora* Lois. *Wetlands* **18**: 35–41.

Pezeshki SR. 2001. Wetland plant responses to soil flooding. *Environmental and Experimental Botany* **46**: 299–312.

R Core Development Team. **2008.** *R: A Language and Environment for Statistical Computing*. Vienna: R Foundation for Statistical Computing.

Rabouille C, Denis L, Dedieu K, Stora G, Lansard B, Grenz C. 2003. Oxygen demand in coastal marine sediments: comparing in situ microelectrodes and laboratory core incubations. *Journal of Experimental Marine Biology and Ecology* **285–286**: 49–69.

Røy H, Lee JS, Jansen S, Beer D De. 2008. Tide-driven deep pore-water flow in intertidal sand flats. *Limnology and Oceanography* **53**: 1521–1530.

Schwarz C, Gourgue O, van Belzen J, Zhu Z, *et al.* 2018. Self-organization of a biogeomorphic landscape controlled by plant life-history traits. *Nature Geoscience* **11**: 672–677.

Strain EMA, van Belzen J, Comandini P, Wong J, Bouma TJ, Airoldi L. 2017. The role of changing climate in driving the shift from perennial grasses to annual succulents in a Mediterranean saltmarsh. *Journal of Ecology* **105**: 1374–1385.

Suding KN, Gross KL, Houseman GR. 2004. Alternative states and positive feedbacks in restoration ecology. *Trends in Ecology and Evolution* **19**: 46–53.

Temmerman S, Bouma TJ, van de Koppel J, van der Wal D, de Vries MD, Herman PMJ. 2007. Vegetation causes channel erosion in a tidal landscape. *Geology* **35**: 631–634.

Ungar IA. 1977. Salinity, temperature, and growth regulator effects on seed germination of *Salicornia europaea L. Aquatic Botany* **3**: 329–335.

Weerman EJ, van de Koppel J, Eppinga MB, Montserrat F, Liu QX, Herman PM. 2010. Spatial self-organization on intertidal mudflats through biophysical stress divergence. *The American Naturalist* **176**: E15–E32.

Wilson CA, Hughes ZJ, FitzGerald DM, Hopkinson CS, Valentine V, Kolker AS. 2014. Saltmarsh pool and tidal creek morphodynamics: dynamic equilibrium of northern latitude saltmarshes? *Geomorphology* **213**: 99–115.

Xie T, Cui B, Li S, Bai J. 2018. Topography regulates edaphic suitability for seedling establishment associated with tidal elevation in coastal salt marshes. *Geoderma* **337**: 1258–1266.

Xin P, Yuan L-R, Li L, Barry DA. 2011. Tidally driven multiscale pore water flow in a creek-marsh system. *Water Resources Research* **47**: W07534, doi: 10.1029/2010WR010110.

Zhu Z, van Belzen J, Zhu Q, van de Koppel J, Bouma TJ. 2019. Vegetation recovery on neighboring tidal flats forms an Achilles' heel of saltmarsh resilience to sea level rise. *Limnology and Oceanography*. doi: 10.1002/lno.11249.